

# An Efficient FTN Implementation of the OFDM/OQAM System

Hao Lin\*, Naila Lahbabi\*†, Pierre Siohan\* and Xiwen Jiang&

\*Orange Labs, Cesson Sévigné, France

†Telecom Bretagne, Brest, France

&Eurecom, Biot, France

**Abstract**—In this paper, we propose an implementation method for Orthogonal Frequency Division Multiplexing Offset Quadrature Amplitude Modulation (OFDM/OQAM) with Faster-Than-Nyquist (FTN) signaling. The proposed scheme can bring several advantages: 1) it approaches the theoretical rate gain of FTN signaling; 2) it can flexibly switch between Nyquist and FTN modes; 3) it does not cause complexity increase for the modem components while switching from Nyquist to FTN mode, and vice versa. In addition, we also present an iterative detector method which can support high constellation order transmission. With the simulations, we intend to show the FTN limits, up to a rate increase by a factor of 2, that the proposed transceiver can reach with various pulse shapes.

## I. INTRODUCTION

The OFDM/OQAM has been presented as a more advanced multicarrier modulation than the OFDM systems because of its high flexibility of waveform utilization; and no cyclic prefix is applied, reaching therefore a full Nyquist rate [1]. Nevertheless, future radio system, such as 5G [2], tends to drive the transmission capacity to its ultimate limit, leading to some novel transmission paradigms. One possibility is to violate the well-known Nyquist condition [3] by transmitting faster than the Nyquist rate, also known as the FTN signaling. In fact, the idea of FTN signaling is not novel and was originally raised by Mazo in 1975 [4]. It was pointed out that the transmission rate is not necessarily limited by the Nyquist rate, meaning that faster transmission rate can be envisaged to trade the interference-free for more throughput. Mazo also showed for Binary Phase Shift Keying (BPSK) that, as long as the boosted transmission rate does not go beyond 1.25x, i.e., a ratio between Nyquist rate and FTN rate, the resulting minimum sequence distance always keeps constant. However, this scheme was not deemed as an attractive means until the trend of the explosion of throughput requirement becomes unavoidable; especially after the extension of combining FTN with OFDM [5]. In addition to the minimum distance, it is proved that FTN can benefit higher capacity from the excess bandwidth of the waveform [6], opening, indeed, a bright door for the waveform design aspect.

An FTN transmitter combined with OFDM/OQAM modulation, called hereafter in short FTN-OQAM, was presented in [7]. The authors introduced a block so-called an FTN mapper to the classical OFDM/OQAM modulator [8]. This block approximates the interference induced from the FTN signaling; then maps them on the symbol level before passing through the OFDM/OQAM modulation. Therefore, the FTN signaling can be flexibly enabled/disabled by switching-on/off the FTN

mapper block. Nevertheless, the FTN mapper introduces additional complexity which highly depends on the interference approximation accuracy, i.e., the more accurate approximation, the more complexity the mapper consumes. Moreover, the interference mapping also necessitates that both the subcarriers on the band edges and the slots on the frame edges shall be reserved as guard band and interval. Thus, the effective transmit rate cannot reach the theoretical rate of FTN signaling. Regarding the detection algorithm, an iterative Maximum A posteriori (MAP)-based receiver, whose complexity increases with the modulation order, is proposed in [9].

In this paper, we present a different FTN-OQAM realization which also can retain the flexibility for switching between FTN and Nyquist modes. Moreover, it does not introduce additional complexity compared with the classical OFDM/OQAM modulation. In addition, its effective rate approaches very closely the one promised by the theory. To deal with the introduced interferences, we propose a receiver based on Minimum Mean Square Error linear equalization and interference cancellation, named MMSE IC-LE. The aim with our system is to boost the transmission rate, which means that high modulation orders will be used. In this respect, the MMSE IC-LE algorithm, whose complexity is independent of the modulation order, turns out to be a good candidate. Since OFDM/OQAM can be equipped with different types of pulse shapes, we propose an algorithm to find, for different modulation orders, the pulse shape providing the ultimate FTN packing factor. The rest of the paper is organized as follows. Section II introduces the background of FTN-OQAM systems. Section III describes our proposed FTN-OQAM transceiver while in Section IV, its performances are evaluated and the FTN limit investigated. Conclusions are given in Section V.

## II. FTN-OQAM BACKGROUND

In this section, we present the background of the OFDM/OQAM followed by a state of the art (SoTA) solution for the FTN-OQAM system.

### A. OFDM/OQAM System

Assuming  $M$  the number of total subcarriers, the continuous-time OFDM/OQAM signal in baseband is [1]:

$$s(t) = \sum_{m=0}^{M-1} \sum_{n=-\infty}^{+\infty} a_{m,n} \underbrace{g\left(t - \frac{nT_0}{2}\right) e^{j2\pi m F_0 t} e^{j\Phi_{m,n}}}_{g_{m,n}(t)}, \quad (1)$$

and its equivalent baseband discrete-time OFDM/OQAM signal is:

$$s[k] = \sum_{m=0}^{M-1} \sum_{n \in \mathbf{Z}} a_{m,n} \underbrace{g[k - nN] e^{\frac{j2\pi m(k - \frac{D}{2})}{M}} e^{j\Phi_{m,n}}}_{g_{m,n}[k]},$$

where  $g_{m,n}$  are called basis functions and construct a Hilbert basis, with  $T_0 F_0 = 1$ , where  $T_0$  is the symbol duration and  $F_0$  is the subcarriers spacing.  $g(t)$  is a prototype function of length  $L$  (without any restrictions, we suppose  $L = bM, b \in \mathbf{Z}$ ),  $N = \frac{M}{2}$  is the discrete time offset,  $D = L - 1$  and  $\Phi_{m,n}$  is a phase term often equal to  $\frac{\pi}{2}(m+n) + \Phi_0$ , where  $\Phi_0 = 0$  or  $\pm\pi mn$ . The real valued transmitted symbol  $a_{m,n}$  on the  $m^{\text{th}}$  carrier at time instant  $n$  is obtained from taking the real and imaginary part of the complex-valued  $2^{2K}$ -QAM constellation. The orthogonality constraint of OFDM/OQAM is expressed using the real inner product as:

$$\Re \left\{ \int_{-\infty}^{+\infty} g_{m,n}(t) g_{m',n'}^*(t) dt \right\} = \delta_{m,m'} \delta_{n,n'},$$

where  $\delta$  is the Kronecker symbol. It is worthwhile noting that this orthogonality condition is satisfied at the Nyquist rate, i.e.  $T_0 F_0 = 1$ .

### B. SoTA solution for FTN-OQAM

FTN consists in reducing the symbol duration or the subcarriers spacing, thus the pulses orthogonality constraints do not longer hold. Theoretically, the baseband FTN-OQAM modulated signal can be written as follows:

$$s(t) = \sum_{m=0}^{M-1} \sum_{n=-\infty}^{+\infty} a_{m,n} g(t - \frac{n\tau T_0}{2}) e^{j2\pi m \zeta F_0 t} e^{j\Phi_{m,n}}, \quad (2)$$

where,  $0 < \tau \leq 1$  and  $0 < \zeta \leq 1$  are the FTN time and frequency packing factors, respectively.

In [7], the authors modify the classical OFDM/OQAM scheme, introducing an FTN time-time frequency lattice with parameters  $(T_\Delta, F_\Delta)$  such that  $T_\Delta = \tau \frac{T_0}{2}$  and  $F_0 = F_\Delta (\zeta = 1)$ . Then, in order to transmit the FTN symbols on the orthogonal basis defined by the Inverse Fast Fourier Transform (IFFT) of the OFDM/OQAM, an additional FTN mapper is introduced. This block performs a projection, of each FTN symbol, into an orthogonal basis functions spanning both time and frequency. Quantitatively speaking, at each FTN symbol position, a zone of neighborhood symbols from orthogonal basis, covering  $\Omega_t$  and  $\Omega_f$  in time and frequency axis, are required for calculation, where the Isotropic Orthogonal Transform Algorithm (IOTA) [1] pulse is used for the OQAM filtering. The FTN mapper is based on the frame processing concept. The slots on the frame edges and the subcarriers on the band edges must be reserved to ensure the projection accuracy. Therefore, this solution cannot approach the theoretical rate improvement due to the buffered slots and subcarriers. Moreover, the FTN mapper introduces an additional complexity which highly depends on the neighborhood zone size for the projection. As to the receiver detection algorithm, in [9], a turbo-like receiver is presented. The inner decoder uses the MAP detection and Soft Interference Cancellation (SIC). However, it is well known that the complexity of an MAP-based equalizer will be significantly increased when the

modulation order increases. This receiver seems to be in favor of transmissions with low modulation order, e.g., BPSK.

### III. PROPOSED FTN-OQAM TRANSCEIVER

The motivation of our investigation is to look for a solution that can retain the advantage of the SoTA solution and at the same time solves the remaining problems. To this end, in this section, we propose a new implementation of the FTN-OQAM modem that fulfills our objectives. Moreover, we present a MMSE IC-LE based iterative receiver instead of the above-mentioned MAP-based equalizer. The reason is simply due to that the complexity of the linear equalizer does not depend on the modulation order.

#### A. Efficient FTN-OQAM modem

Similar to [7], we assume that the FTN is realized by packing the pulses closer in time domain ( $\zeta = 1$ ). Thus, (2) can be written in its discrete-time version as

$$s[k] = \sum_{n=0}^{+\infty} g[k - nN_f] \times \underbrace{\sum_{m=0}^{M-1} a_{m,n} e^{j\Phi_{m,n}} e^{\frac{j2\pi m(nN_f - \frac{D}{2})}{M}} e^{\frac{j2\pi m(k - nN_f)}{M}}}_{\text{Pre-processing}} \underbrace{\hspace{10em}}_{\text{IFFT+CYCEXD}}$$

where the FTN factor is denoted as  $N_f = \lfloor \tau \cdot \frac{M}{2} \rfloor$  with  $\lfloor \cdot \rfloor$  the floor function. The prototype filter  $g[k]$  is causal  $k \in [0, L - 1]$ . The modulator is implemented using the IFFT, and thanks to its periodicity property, the filtering is realized using a cyclic extension per block, followed by a multiplication with a single coefficient and finally by a Parallel-to-Serial (P/S) conversion as shown in Fig. 1. The cyclic extension block, named **CYCEXD** can be expressed in the following

$$L \times M \text{ matrix form: } \mathbf{CYCEXD}_{L \times M} = \begin{bmatrix} \mathbf{I}_{M \times M} & & \\ & \dots & \\ & & \mathbf{I}_{M \times M} \end{bmatrix}_{L \times M},$$

where  $\mathbf{I}_{M \times M}$  is the  $M$ -size identity matrix.

The demodulator performs the dual operations of the modulator. Fig. 2 presents the FTN-OQAM demodulator structure. The inverse operation of the **CYCEXD** is performed by the receiver by a block named **CYCCOMB**:

$\mathbf{CYCCOMB}_{M \times L} = \mathbf{CYCEXD}_{L \times M}^T$ , where  $(\cdot)^T$  denotes transposition.

The proposed modem can produce OFDM/OQAM modulation at both Nyquist and FTN rates, simply by adjusting the packing factor  $N_f$ . As to the arithmetic complexity of our modem, there is no complexity increase when switching from Nyquist mode to FTN mode, and its complexity is analogue with the classical OFDM/OQAM modem [8], although the way of implementation is different. Further complexity reduction algorithm, such as [10], can also be readily applied in our modem. Theoretically, for a compressing factor  $\tau$  between 0 and 1, the transmission rate for a FTN transceiver is expected to be multiplied with  $\frac{1}{\tau}$ . Thus the rate growth is a hyperbolic function of  $\tau$ . We compared the effective rate improvement of our proposed modem with the one of [7] assuming that one frame contains 16 symbols;  $M = 128$ ;  $F_\Delta = 1$ ;  $(T_\Delta, \tau) \in [0.4, 0.9]$ , and  $\Omega_t = \Omega_f = 3$ .

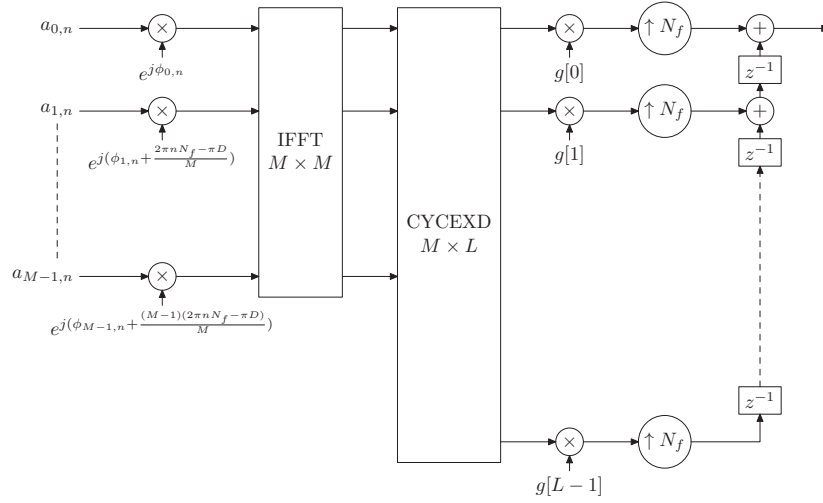


Fig. 1: FTN-OQAM modulator.

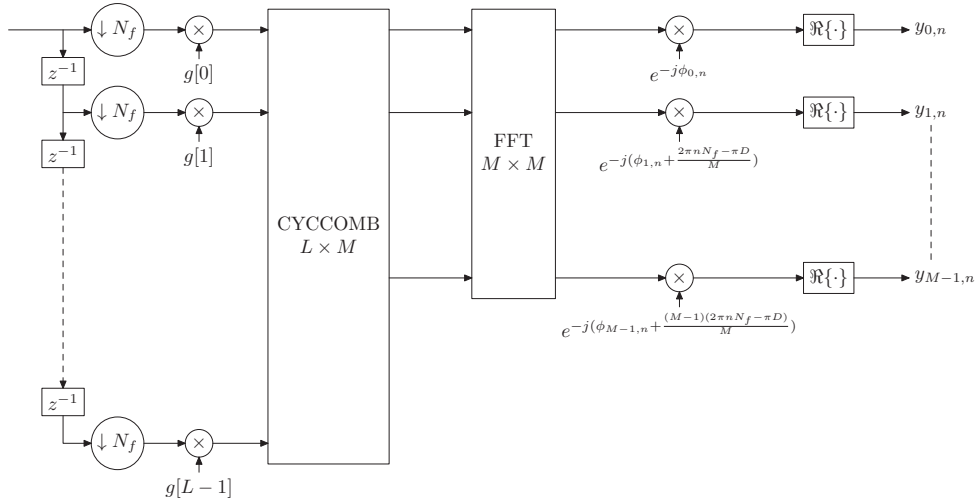


Fig. 2: FTN-OQAM demodulator.

As shown in Fig.3, it is clear that, compared with the SoTA solution, the effective rate improvement of our modem approaches very more closely the theoretical curve. Note that using the same construction principle, we can also build an FTN-OFDM/QAM modem for the direct transmission of complex QAM symbols. In this case, the FTN factor is defined as:  $N_f = \lfloor \tau \cdot M \rfloor$ .

### B. MMSE IC-LE based receiver

The FTN-OQAM transmission chain is reported in Fig. 4. On the transmitter side, coded symbols are modulated through the FTN-OQAM modulator, while on the receiver side, Soft-In-Soft-Out (SISO) MMSE IC-LE is used after demodulation to iteratively suppress the interferences caused by FTN. Instead of a MAP-based equalizer, here we consider a low complexity linear MMSE equalizer that enables high modulation order. Though the pulses are only packed in time, Inter-Carrier Interference (ICI) still exists in the transmitted signal.

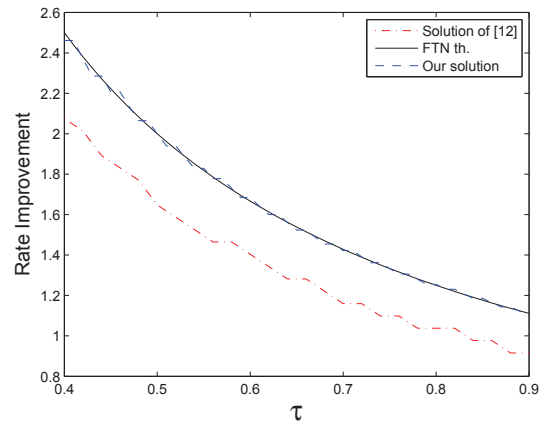


Fig. 3: The rate improvement of FTN-OQAM in function of  $\tau$  using different implementations.

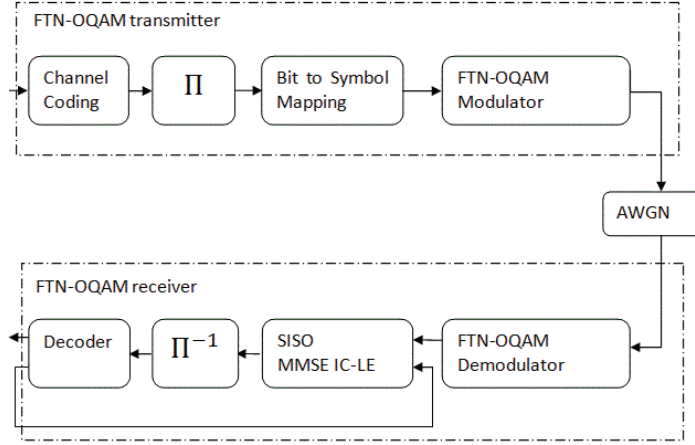


Fig. 4: FTN-OQAM transmission chain.

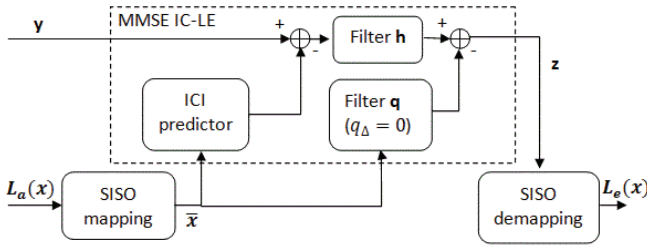


Fig. 5: Structure of the SISO MMSE IC-LE.

The interference cancellation is a 2-stage process, meaning that it cancels Inter-Symbol Interference (ISI) in the first stage and then addresses ICI. Fig. 5 describes the structure of the inner SISO MMSE-IC-LE where ICI and ISI are predicted using the feedback from decoder and then canceled, respectively. The linear filters  $\mathbf{h}$  and  $\mathbf{q}$  coefficients are computed according to the MMSE principle, [11, Chp. 11]. The soft mapping and demapping functions are used to translate the information from bit level to symbol level and vice-versa and thus exchange information between the symbol level filter and the bit level decoder. In Fig. 6, let the red triangle be the targeted element to be equalized. The ICI affecting it is then calculated by the ICI predictor block using the blue triangles which represent the estimated data on side subcarriers. The ISI is predicted using the estimated data on the same subcarrier at different time instants, represented here by the orange triangles. Such a scheme is called time-domain equalization and interference canceling.

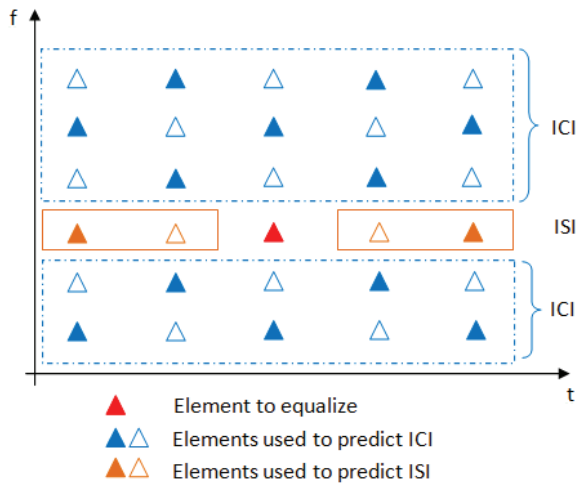


Fig. 6: Time domain ICI and ISI prediction and canceling.

#### IV. SIMULATION RESULTS

In this section, we first give the simulation results of the efficiency of transceiver, proving that our proposed transceiver can support high modulation order transmission. Then we present the methodology with which we can investigate the FTN limit of our transceiver.

##### A. Transceiver validation

In our simulation, we assume the number of subcarrier is  $M = 128$  and all the subcarriers are to be modulated. The modulation order is set to 64-QAM. The frame is composed of 20 complex symbol slots which corresponds to 15360 coded bits. The outer code used is a (1,5/7) Recursive Systematic Convolutional code. The prototype filter used is the Frequency Selective (FS) one [12] with filter length =  $4M$ . The interleaver is assumed to be random. On the receiver side, the MMSE filter has length of 30 coefficients. The outer decoder is based on MaxLogMap algorithm [11]. The simulation results, in terms of Bit Error Rate (BER) versus Signal to Noise Ratio (SNR), are given in Fig. 7 for the packing factor of 0.8. The results show a good BER convergence between the

FTN signaling and Nyquist signaling after 7 iterations. This proves the effectiveness of our proposed transceiver even for high modulation order case.

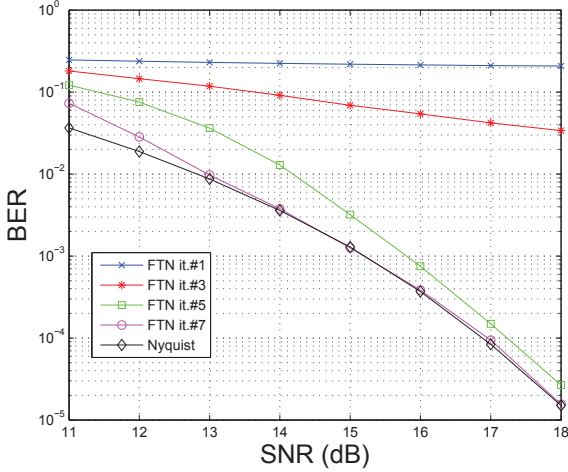


Fig. 7: BER evaluation for proposed FTN-OQAM transceiver, 64-QAM, FS4 filter and FTN packing factor = 0.8.

### B. FTN limit investigation

As for OFDM/OQAM, the FTN-OQAM transceiver can operate with pulse shapes having different time-frequency localization features. In this section, we look for the ultimate limit that FTN-OQAM system can address. By ultimate limit, we mean the smallest packing factor for which we can nearly reach the performance of Nyquist signaling for a given pulse shape and modulation order. To this end, we ignore the restriction on the number of iterations. The methodology of the FTN limit search is summarized in Fig. 8. We indeed repeatedly implement this method for different pulse shape and modulation order. The receiver technique sticks to the aforementioned MMSE IC-LE. The simulation tool used is the EXtrinsic Information Transfer (EXIT) chart due to two main advantages [13]: 1) it reflects a BER vs. SNR prediction; 2) it is less time consuming than BER simulation.

The target convergence performance with Nyquist signaling is fixed at BER of  $10^{-5}$ , which is the Nyquist Error-Free (NEF) in the sequel. The search process begins by generating the SNR value corresponding to the NEF point and initializing the FTN packing factor to 0.1. Using these values, the EXIT chart is generated. If the EXIT tunnel is closed or the EXIT chart does not reach NEF, the packing factor is incremented by a certain step and the previous operation is repeated. The iterative process continues until the EXIT tunnel is open and the EXIT chart reaches NEF, e.g., see Fig. 9. Note that the precision of our FTN limit estimation depends on the step value.

In what follows, we present the FTN limit investigation only for the IOTA pulse shape with filter length =  $4M$  (IOTA4) as an example. According to our BER vs. SNR simulation with IOTA4 pulse shape, the SNR corresponding to NEF yields 6.2 dB, 12.6 dB and 18.3 dB for QPSK, 16-QAM and 64-QAM, respectively. It is also worth noting that in

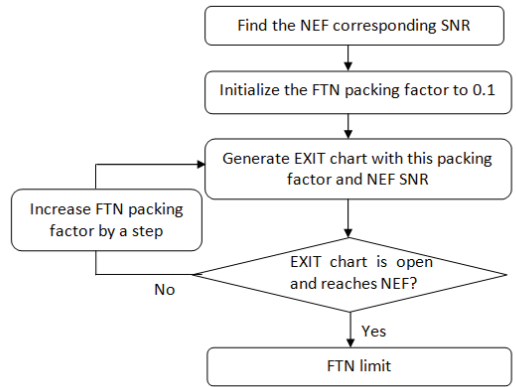


Fig. 8: Search process to find FTN limit.

the AWGN case, different pulse shapes with Nyquist signaling always lead to identical BER performance.

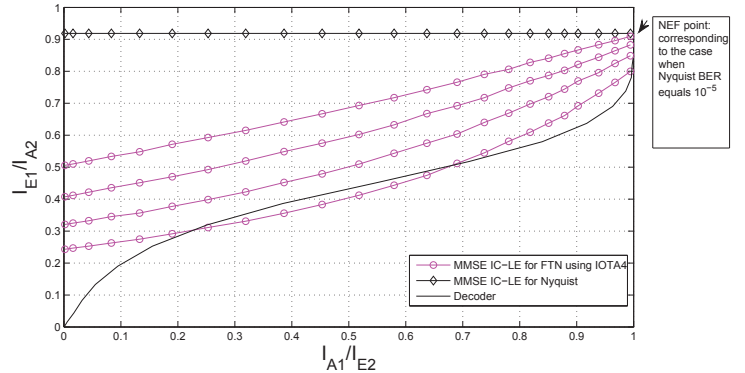


Fig. 9: EXIT chart for MMSE IC-LE with QPSK using IOTA4 at SNR= 6.2 dB. The FTN packing factor ranges from 0.3 (bottom) to 0.6 (top) in step of 0.1.

In Fig. 9, we see that the EXIT chart starts to open for a packing factor between 0.3 and 0.4, meaning that the iterative process begins to converge. At FTN packing factor of 0.6, the intersection point of MMSE IC-LE and the decoder almost reaches the one of the Nyquist case, i.e. our FTN-OQAM receiver converges to the Nyquist performance. Thus, the FTN packing factor of 0.6 is identified as the FTN limit for QPSK using IOTA4. Figs. 10 and 11 report the EXIT charts for 16-QAM and 64-QAM, respectively, showing FTN limits equal to 0.8 for 16-QAM and between 0.9 and 1.0 for 64-QAM.

Same search process is carried out for other pulse shapes: the Square Root Raised Cosine filter of length  $4M$  (SRRC4) with different roll-off (RO) factors; the PHYDYAS filter [14] with length  $4M$  (PHYDYAS4); the Time Frequency Localization prototype filter [12] with length  $M$  (TFL1); and the Extended Gaussian Function [8] with length  $4M$  (EGF4) and spreading factor 2. The results summarized in Tab. I show that a rate improvement up to a factor of 2 is feasible with FTN signaling. While Tab. II reports the recommendations on the

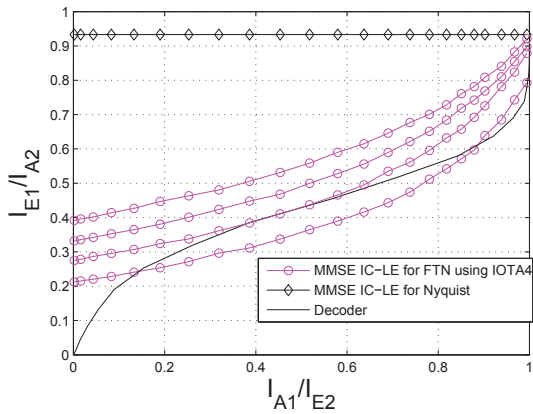


Fig. 10: EXIT chart for MMSE IC-LE with 16-QAM using IOTA4 at SNR= 12.6 dB. The FTN packing factor ranges from 0.5 (bottom) to 0.8 (top) in steps of 0.1.

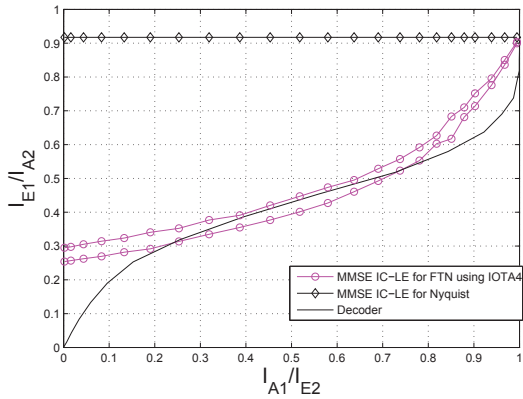


Fig. 11: EXIT chart for MMSE IC-LE with 64-QAM using IOTA4 at SNR= 18.3 dB. The FTN packing factor ranges from 0.8 (bottom) to 0.9 (top) in steps of 0.1.

pulse shapes for different FTN factors and modulation orders. This could eventually be useful when one considers the pulse shape adaptation.

Pulse shapes	QPSK	16-QAM	64-QAM
SRRC4 (RO=0.3)	0.9	> 0.9	> 0.9
SRRC4 (RO=0.5)	0.8	0.9	0.9
PHYDYAS4	0.8	0.9	0.9
FS4	0.7	0.9	0.9
IOTA4	0.6	0.8	> 0.9
TFL1	0.5	0.7	> 0.9
EGF4	0.5	0.8	> 0.9

TABLE I: FTN limit for different pulse shapes and modulation orders.

## V. CONCLUSION

In this paper, we presented a FTN-OQAM transceiver which, differently from the SoTA solution, very closely approaches the FTN theoretical rate growth and it does not result

	FTN limit	Recommend pulse	Rate growth
QPSK	0.5	TFL1/EGF4	2
16-QAM	0.7	TFL1	1.43
64-QAM	0.9	SRRC4(RO=0.5)/PHYDYAS4/FS4	1.11

TABLE II: FTN limit for different modulation orders and recommended pulses.

in additional complexity increase when switching from the Nyquist mode to the FTN mode. Moreover, an MMSE-LE-IC-based iterative receiver was presented instead of a MAP-based equalizer. By simulations, it confirmed that the proposed transceiver can support the transmission with high modulation order. Further, the FTN limits of the proposed transceiver were investigated and reported. The suitable pulse shapes were recommended; such information is useful for a system considering pulse shape adaptation. This will be studied more in detail in our future work.

## ACKNOWLEDGMENT

This work has been performed in the framework of the FP7 project ICT-317669 METIS. The authors would like to acknowledge the contributions of their colleagues. Moreover, the authors would like to thank Raphaël LE BIDAN and Christophe LAOT of Telecom Bretagne for the valuable discussions.

## REFERENCES

- [1] B. Le Floch, M. Alard, and C. Berrou. "Coded Orthogonal Frequency Division Multiplex". Proceedings of the IEEE, vol. 83, pp. 982-996, June 1995.
- [2] "Mobile and Wireless communications enabler for the twenty-twenty information society". <https://metis2020.com/>.
- [3] H. Nyquist. "Certain topics in telegraph transmission theory". Trans. AIEE, vol. 47, pp.617-644, Apr. 1928.
- [4] E. Mazo. "Faster-Than-Nyquist signaling". Bell. Syst. Tech. Journal, 54:1451-1462, 1975.
- [5] J.B. Anderson and F. Rusek. "Improving OFDM: Multistream Faster-Than-Nyquist Signaling". In Turbo Codes Related Topics; 6th International ITG-Conference on Source and Channel Coding (TURBOCODING), 2006 4th International Symposium, pp. 1-5, Apr. 2006.
- [6] F. Rusek and J.B. Anderson. "Constrained Capacities for Faster-Than-Nyquist Signaling". Information Theory, IEEE Trans, vol. 55, no. 2, pp. 764-775, Feb. 2009.
- [7] D. Dasalukunte, F. Rusek and J.B. Anderson. "Transmitter architecture for Faster-Than-Nyquist signaling systems". In Circuits and Systems, 2009. ISCAS 2009. IEEE International Symposium, pp. 1028-1031, May. 2009.
- [8] P. Siohan, C. Siclet and N. Lacaille. "Analysis and design of OFDM/OQAM systems based on filterbank theory". IEEE Trans. Signal Process, vol. 50, no. 5, pp. 1170-1183, 2002.
- [9] D. Dasalukunte, F. Rusek, V. Owall. "An Iterative Decoder for Multicarrier Faster-Than-Nyquist Signaling Systems". In Communication (ICC), 2010. IEEE International Conference, pp. 1-5, May. 2010.
- [10] Y. Dandach, and P. Siohan. "FBMC/OQAM modulators with half complexity". In Proceedings Globecom'11 (Houston, USA), Dec. 2011.
- [11] C. Berrou. "Codes and turbo codes". Springer-Verlag France, 2010.
- [12] D. Pinchon, P. Siohan, and C. Siclet. "Design techniques for orthogonal modulated filterbanks based on a compact representation". IEEE Trans. Signal Process, vol. 52, no. 6, pp. 1682-1692, 2004.
- [13] S. Ten Brink. "Convergence of iterative decoding". Electron. Lett, vol. 35, no. 13, pp. 1117-1119, Jun. 1999.
- [14] M. Bellanger. "Specification and design of a prototype filter for filter bank based multicarrier transmission". ICASSP, 2001.